RESEARCH-ARTICLE

Distinguishing Adaptive Search from Random Search in Robots and T cells

GEORGE MATTHEW FRICKE, The University of New Mexico, Albuquerque, NM, United States

SARAH R BLACK, The University of New Mexico, Albuquerque, NM, United States

JOSHUA PETER HECKER, The University of New Mexico, Albuquerque, NM, United States

JUDY L CANNON, The University of New Mexico, Albuquerque, NM, United States

MELANIE E MOSES, The University of New Mexico, Albuquerque, NM, United States

Published: 11 July 2015

GECCO '15: Genetic and Evolutionary Computation Conference
July 11 - 15, 2015
Madrid, Spain

Conference Sponsors:
SIGEVO

https://doi.org/10.1145/2739480.2754794
ISBN: 9781450334723

Distinguishing Adaptive Search From Random Search in Robots and T cells

G. Matthew Fricke
Computer Science Dept.
The University of New Mexico
Albuquerque, NM USA
mfricke@cs.unm.edu

Sarah R. Black
Dept. of Mathematics
The University of New Mexico
Albuquerque, NM USA
sarblack92@gmail.com

Joshua P. Hecker
Computer Science Dept.
The University of New Mexico
Albuquerque, NM USA
jhecker@cs.unm.edu

Judy L. Cannon
Dept. of Molecular Genetics
and Microbiology
and Dept. of Pathology
The University of New Mexico
Albuquerque, NM USA
jucannon@salud.unm.edu

Melanie E. Moses
Depts. of Computer Science
and of Biology
The University of New Mexico
Albuquerque, NM USA
Santa Fe Institute
melaniem@cs.unm.edu

ABSTRACT

In order to trigger an adaptive immune response, T cells move through lymph nodes (LNs) searching for dendritic cells (DCs) that carry antigens indicative of infection. We hypothesize that T cells adapt to cues in the LN environment to increase search efficiency. We test this hypothesis by identifying locations that are visited by T cells more frequently than a random model of search would suggest. We then test whether T cells that visit such locations have different movement patterns than other T cells. Our analysis suggests that T cells do adapt their movement in response to cues that may indicate the locations of DC targets. We test the ability of our method to identify frequently visited sites in T cells and in a swarm of simulated iAnt robots evolved to search using a suite of biologically-inspired behaviours. We compare the movement of T cells and robots that repeatedly sample the same locations in space with the movement of agents that do not resample space in order to understand whether repeated sampling alters movement. Our analysis suggests that specific environmental cues can be inferred from the movement of T cells. While the precise identity of these cues remains unknown, comparing adaptive search strategies of robots to the movement patterns of T cells lends insights into search efficiency in both systems.

Categories and Subject Descriptors

I.2.9 [**Artificial Intelligence**]: Robots—*Autonomous vehicles*; F.2.2 [**Theory of Computation**]: Nonnumerical Algorithms and Problems—*Sorting and searching*

GECCO '15, July 11 - 15, 2015, Madrid, Spain
 ISBN 978-1-4503-3472-3/15/07…$15.00
DOI: http://dx.doi.org/10.1145/2739480.2754794

Keywords

swarm robotics; robot search; immunological search; evolutionary computation

1. INTRODUCTION

Identifying algorithms and behaviours for effective distributed search without centralized coordination is a challenging computational problem, particularly important for distributed systems such as wireless sensor networks and swarm robotics. Complex biological systems have evolved spectacularly successful decentralized collective search, exemplified by ant colonies and immune systems. Ant colonies with millions of individuals collectively forage in dynamic landscapes without hierarchy or centralized control; their decentralized foraging strategies have dominated resource consumption in challenging and dynamic environments across the globe for over 100 million years [22]. Immune systems comprised of trillions of cells differentiated into dozens of cell types are forced by an evolutionary arms race to rapidly find and eradicate previously unseen pathogens, with each cell acting independently of any centralized controller.

A goal of artificial immune systems is to emulate biological strategies in computational systems; however, the mechanisms that generate adaptive biological search are not always well understood. In this paper we use computational tools to infer whether certain cells of the immune system search randomly or whether they adapt to their search environment to search more efficiently. We then compare movement patterns during search in the immune system to decentralized search in robotic swarms whose behaviour was inspired by foraging ants. Our robots adapt to sensed features of their environment to improve search efficiency. Here we ask whether T cells similarly adapt to features of their environment during search. By studying both systems in the same framework, we gain insights into distributed search in both immunology and swarm robotics. Additionally, we improve our understanding of the movement patterns of searching T cells, thereby identifying potential mechanisms for distributed search in robotics.

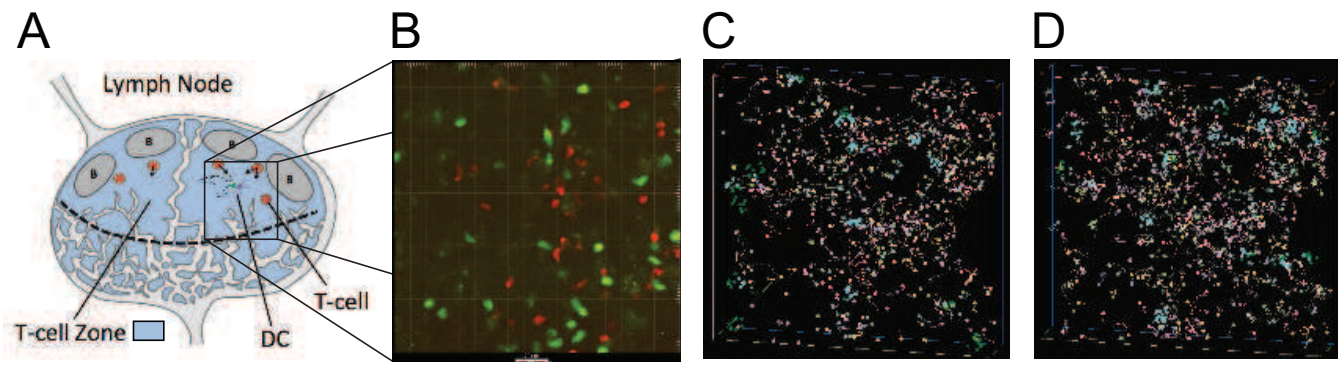

Figure 1: A) Diagram of a LN with T cell zone shown in blue. B) Observation field. $350 \times 350 \times 70\mu$m 2PM image of a region in the T cell zone with T cells tagged with red and green dyes. C) Observed T cell tracks; simulated DCs are in cyan (discovered) and magenta (undiscovered), all other colours are T cell tracks. D) The model generated set of tracks; starting positions are the same as the observed T cells.

1.1 T cell Search for DCs in LNs

In this paper, we focus on a search process which is crucial for the initiation of an adaptive immune response: the search for antigen-bearing dendritic cells (DCs) by T cells in LNs. In order to mount an effective immune response, T cells must be activated in LNs (Fig.1A). Antigens are markers that identify particular pathogens, and each T cell matches a particular set of antigens. A DC presenting an antigen indicates that the corresponding pathogen has been encountered in the organism's tissues. T cell interactions with DCs displaying cognate antigen are necessary to trigger an adaptive immune response [15].

To facilitate T cell activation, T cells and DCs interact within the T cell zone of LNs. The T cell zone is on the order of $1\,\text{mm}^3$ in the inguinal mouse LNs we analyse. T cells and DCs are on the order of $10\,\mu$m in diameter, so each T cell must search a space 1 million times its own volume in each lymph node. In secondary lymphoid organs, DCs usually comprise between 1% and 5% of the T cell zone's total cell population. Each T cell interacts with as many DCs as possible in order to maximize the probability of detecting a matching antigen [17]. This imposes the need for efficient random search to mount an effective immune response.

Early response to infection depends on the rate at which DCs are encountered by T cells in the lymph node. The adaptive immune system is in an evolutionary arms race against an exponentially-growing pathogen population. That evolutionary pressure selects for efficient detection of, and response to, infection [11]. Therefore we hypothesise that evolutionary pressure has produced an efficient mechanism for bringing T cells and DCs together, providing a model that can be used for random robotic search and in which we can explore the efficiency of the observed T cell search.

Two-photon microscopy (2PM) has allowed a revolution in the observation and tracking of cell movement in intact tissues. We use 2PM to study T cell movement in a LN that has been excised from a mouse. In this ex vivo experiment, T cells remain alive and motile and their movement is visualized with 2PM. Laser light scanning through the ex vivo LN cause molecules bound to T cells to fluoresce at a particular wavelength. These fluorescence signals are are localized in 3-dimensions producing a position in space and time for individual T cells. Knowing the positions of T cells and the frame rate of image capture, we can also calculate T cell speeds and step lengths.

1.2 Adaptive and Stochastic Search Strategies

While 2PM provides abundant T cell movement data, it can be difficult to determine whether cells are responding to local information or are employing a purely stochastic search strategy. We describe a method of analysing search patterns in T cells that allows us to distinguish adaptive search from purely stochastic search.

Stochastic spatial search is a task common to biological and engineered agents. In environments where target distributions are unknown or change over time randomized search strategies are more effective than deterministic strategies [1, 19]. Here we identify two kinds of non-deterministic search strategies: adaptive strategies that change in response to features of their environment and purely stochastic strategies that do not. Searchers employing an adaptive strategy sample the distribution of targets as they are encountered and use the information gained to create an informed search strategy. For example *Escherichia coli* couple their flagella motility and sensors through an integrative feedback loop in their signal transduction network. This causes *E. coli* to either *tumble* or *run* in space depending on whether they are moving up or down a chemoattractant gradient. As a result *E. coli* tend to move to, and remain in, the most resource rich parts of their environment [3].

Searchers using purely stochastic strategies form a pattern of movement by sampling from probability density functions (PDFs) that govern turning angles and step lengths. For example, *Paenibacillus dendritiformis* posess internal clocks that allow changes in direction independent of environmental cues [4]. Viswanathan et al. characterized the movement of *Diomedea exulans* [21], and Humphries et al. described *Thalassarche melanophrys* [13] searching for pelagic prey as statistically driven, where the pattern of motion is fractal, that is the distribution of step lengths is similar at all scales, defined as a Lévy flight. Such search patterns are provably optimal when targets are rare and are not permanently depleted when discovered.

Motion in general can be described as a sequence of positions over time. We define *step length* to be the shortest distance between positions after merging all positions where the angle turned since the last position is less than 15°.

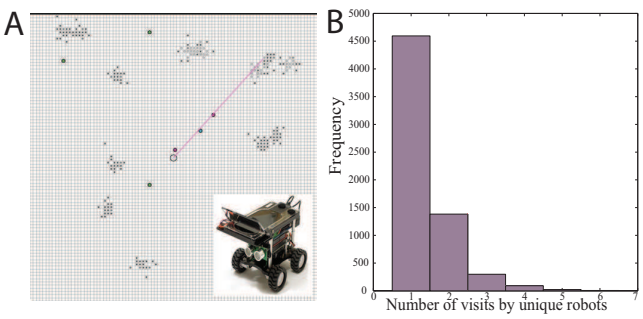

Figure 2: A) An image of an iAnt robot (inset) and a simulation of 6 iAnts foraging for clustered targets. B) Distribution of the number of different iAnt robots that visit each 8 cm^2 grid cell during the search phase of simulated foraging.

The mean squared displacement of a simple random walk (Brownian motion) grows as the square root of time and on 2-dimensional surfaces Brownian motion is space filling [20]. The result is a pattern of motion that is very *thorough* in that it visits all nearby locations eventually, but expands the search area (*extent*) relatively slowly. In contrast Lévy walks are less thorough but they are superdiffusive with displacement exceeding that of Brownian motion until the limit of ballistic (straight line) motion is reached. Brownian motion is therefore more efficient at finding local, densely packed targets. Lévy walks tend to be more efficient when targets are sparsely distributed in space [21]. The optimal tradeoff between thoroughness and extent depends, in part, on the distribution of targets.

Harris et al. [9] describe the movement patterns of T cells searching for *Toxoplasma gondii* and find that they are consistent with a Lévy flight. Our prior analysis of T cell movement in the LN also suggested a Lévy pattern of search, however more detailed analysis of additional data suggests the pattern of motion of T cells searching for DCs is a combination of a correlated random walk (CRW), and steps drawn from a lognormal PDF.

1.3 iAnt Robot Swarms

iAnt robots swarms provide a platform for experiments in biological search in an embodied robotic system [14]. iAnts are built from commodity parts including an ultrasonic rangefinder, a compass, and 2 cameras. An Arduino Uno microcontroller and iPod touch provide for onboard computation and sensor integration. (Fig. 2A, inset).

The robots implement an ant-inspired central place foraging algorithm (CPFA) that mimic colonies of seed-harvester ants using a combination of individual memory and pheromone trails to efficiently collect clustered resources and carry them to a central nest. The iAnt CPFA is based in field observations of seed harvester ants [5]. iAnt behaviour has several phases, including, and of primary significance to this work, adaptive and uninformed statistical random search phases. An agent-based simulation replicates the movement and sensing capabilities of these robots. A genetic algorithm (GA) evolves parameters that control the sensitivity threshold for triggering behaviours, the likelihood of transitioning from one behaviour to another, and the length of time each behaviour should last. In this work we analyse data from a simulation, which is carefully parametrised to reflect the behaviour, sensing, and navigation error of physical iAnt robots [10].

2. METHODS

2.1 T cell Observations

Lymph nodes (LNs) were prepared according to the protocol described previously by Matheu, Parker and Cahalan [16]. T cells were purified by nylon wool according to Allenspach et al. [2] and labelled with fluorescent dyes, and then between 5 and 10 million labelled T cells were injected intravenously into recipient mice. Fifteen to 18 hours later, after T cells migrated into LNs, the inguinal LNs were removed and recorded using two-photon microscopy (2PM). Imaging experiments were performed using the methods described in Fricke at al. [6]. This observation (Fig. 1B) provides the data needed to develop a statistical model of T cell search, informed the simulations of T cells search (Fig. 1D), and allow us to detect deviations between observation and simulation. We detail the analysis of the movement of 438 T cell tracks, consisting of 11,951 positions, in one experimental observation of a LN. We also provide summary statistics that characterize T cell movement in an additional 40 experimental LN observations.

2.2 T cell Model

In other work we built a simulation in which T cells move stochastically and match the statistical properties of observed T cell motion. Simulated T cells moved using a purely stochastic search derived from fitting probability density functions (PDFs) to the the observed T cell tracks using maximum likelihood estimation (MLE). Here the simulation serves as the null model (H_0) in which T cells do not adapt to their environment. The simulation is implemented as a continuous (floating-point) 3D model written in C++. Our observations have an average volume of 6.3×10^6 μm^3. T cell tracks were observed and recorded as 3D coordinate sequences within a bounding box defined by the visible section of the ex vivo lymph node. Simulations of the observed field were repeated 10 times. Searchers in the idealized model start at the same initial positions as the observed T cells, and exist in a volume equal to the observed field volume (Fig. 1). Each T cell track in a simulated field corresponded to a T cell track in the observed field. T cells in the simulated field were constrained to move a total distance equal to the distance covered by the observed T cells. A T cell was considered to have encountered a DC if the distance between a T cell and a DC was less than 10 µm. T cells and DCs were modelled as spheres with diameter 10 µm.

2.3 Identifying Hot Spots

The field was discretised into 8000 μm^3 voxels (the length of a voxel is 20 µm, approximately twice the diameter of a T cell). For each voxel in the field, we count how many times that location was visited by distinct T cell tracks. We defined *hot spots* as locations that are visited by more T cell tracks than would be predicted by the null model (H_0).

Hot spots were determined by the following method. We calculated the number of unique track visits to each location in each simulation, repeating the simulation of the observed LN 10 times. We then took the average of the maximum number of unique track visits to locations over the simulations. This is the H_0 prediction for the maximum number of

visits to any location using a purely stochastic search. Let x be the maximum number of visits predicted by H_0. The locations in the observed LN were filtered so that only locations visited more than x times were identified as hot spots. Fig. 3A shows the distribution of the number of unique T cells that step into each voxel for the 10 simulations of one LN and the empirical observation from that same LN. In the LN shown in Fig. 3, any location visited 8 times or more was identified as a hot spot.

T cell tracks that visit any hot spot at any time during the observation were identified as hot tracks. We call all other tracks cold tracks.

2.4 Search in Robot Swarms

In this paper we analyse data from simulated iAnts, focusing on one aspect of adaptive iAnt foraging behaviour: robot movement during the search phase of foraging. iAnts have 2 search modalities: informed and uninformed correlated random walks (CRWs).

Search using an *uninformed walk*: the robot has no information about the location of targets. In this case it searches using a correlated random walk with fixed step size and direction θ_t at time t, defined by Equation 1:

$$\theta_t = \mathcal{N}(\theta_{t-1}, \sigma) \tag{1}$$

Where $\mathcal{N}(\mu, \sigma)$ is a Gaussian PDF with mean, μ, and standard deviation, σ. The standard deviation, σ, determines how correlated the direction of the next step is with the direction of the previous step. Robots initially search for resources using an uninformed correlated random walk, where σ is assigned a fixed value in Equation 2:

$$\sigma \leftarrow \omega \tag{2}$$

where the value of ω is evolved to maximize foraging efficiency by a genetic algorithm (GA).

Search using an *informed walk*: If the robot is informed about the location of resources (because of its own memory of previously discovered targets or because of pheromone communication from another robot), it searches using an informed CRW, where the standard deviation σ is defined by Equation 3:

$$\sigma = \omega + (4\pi - \omega)e^{-\lambda_{id}t} \tag{3}$$

The standard deviation of the successive turning angles of the informed random walk decays as a function of time t, producing an initially undirected and localized search that becomes more correlated over time. This time decay allows the robot to search thoroughly where it expects to find targets, but also to straighten its path, increase displacement, and so search more broadly if a target is not found. If the robot discovers a target, it transitions to sensing the local target density. The higher the local density of targets the higher the probability that the iAnt transitions to using an informed rather than an uninformed CRW.

2.5 iAnt GA and Experimental Design

We evolved a population of 100 simulated robot swarms for 100 generations, though convergence consistently occurred in fewer generations. Fitness was defined as the number of targets detected by the robot swarm in one hour of simulated time. We used the recombination and mutation described in our previous work [14]. Parameters were randomly initialized using independent samples for each swarm. Robots within a swarm used identical parameters throughout the hour-long simulation. During each generation of the GA, all 100 swarms underwent 8 fitness evaluations, each with different random placements of 256 targets into 4 clusters. A new random placement of targets was performed for each fitness evaluation.

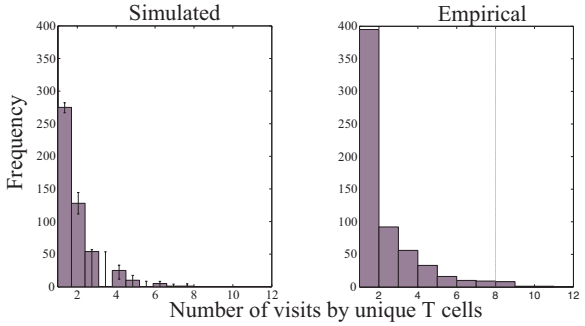

Figure 3: Distribution of the number of unique T cells that visit each of 800 voxels in space A) averaged over 10 simulations (standard deviations shown as error bars) and B) empirically in 1 observation window of a LN. Sites visited 10 or more times (indicated by the red line) are considered frequently visited hot spots.

At the end of each generation, the fitness of each swarm was the sum total of targets collected in the 8 runs of a generation. Deterministic tournament selection with replacement (tournament size = 2) was used to select 99 candidate swarm pairs. Each pair was recombined using uniform crossover and 10% Gaussian mutation with fixed standard deviation (0.05) to produce a new swarm population. We used elitism to copy the swarm with the highest fitness, unaltered, to the new population – the resulting 100 swarms made up the next generation.

We used the highest fitness parameter set from 10 runs of the GA to determine parameters in Equations 1, 2 and 3. We then ran experiments in simulation to generate iAnt movement data which we analysed and compared to T cell movement. All experiments were simulations of 6 iAnt robots searching for 256 targets arranged into 4 clusters. Physical iAnts have an $8\,\mathrm{cm}^2$ detection area and explored a $100\,\mathrm{m}^2$ area for 1 h. The simulated arena reproduces these dimensions.

3. RESULTS

3.1 Analysis of T cell Hot Spots

Our goal is to identify whether T cells modify their movement in response to local features of the lymph node (LN) environment, and if so, if those modifications appear to be adapted to increase search efficiency. First we identify hot spots that are visited by T cells more frequently than is expected by our null model. This expectation is produced by 10 repeated simulations that contain no adaptive movement (Fig. 3). We then characterize the movement of the T cell tracks that visit those hot spots to determine if T cells visiting hot spots move differently than T cells that do not visit hot spots.

The counts of unique T cells visiting each voxel are shown in Fig. 3. The hot spots of one LN along with the T cells that visited those hot spots are visualized in Fig. 4.

We calculated the step length distribution of the T cells

Table 1: **Comparison of the distribution of step lengths of hot T cell tracks (those that visit hot spots) and cold tracks (those that do not visit hot spots).** In order to compare the 514 hot tracks to the 4,998 cold tracks we randomly select five sets of 514 uniformly chosen tracks and show the 95% confidence interval (CI) for each cold track statistic. Bold table columns indicate hot track statistics (the median, variance, skew and kurtosis) that are outside of the 95% CI of cold tracks. While the mean step length for hot tracks does not fall out of the cold track 95% CI, the significantly smaller variance, skew and kurtosis of hot tracks reinforce that hot tracks are less heavy tailed than cold tracks and therefore exhibit a more Brownian pattern of motion.

	Mean	Median	Variance	Skew	Kurtosis
Hot Tracks	2.84 µm	**2.12 µm**	**8.71 µm^2**	**5.37**	**54.8**
Cold Tracks	3.01±0.67 µm	1.71±0.0979 µm	182±129 µm^2	17.2 ± 6.3	332 ± 221

Table 2: **Comparison of the distribution of step lengths of informed iAnts (those revisiting known resource locations) and uninformed iAnts (those searching without knowledge of resource locations).** The informed tracks have mean and median step lengths that are shorter than the 95% CI of uninformed tracks, while the variance, skew and kurtosis of hot tracks are within the 95% CI of uninformed tracks.

	Mean	Median	Variance	Skew	Kurtosis
Informed Tracks	**1.95 m**	**1.7 m**	2.6 m^2	1.29	5.03
Uninformed Tracks	2.84±0.16 m	2.83±0.133 m	2.45±1.2 m^2	1.08 ± 0.617	5.42 ± 1.18

that visit hot spots (shown in color in Fig. 4) and those that do not visit any hot spots (in gray).

T cell steps lengths are constructed by converting a sequence of positions in a T cell track into a sequence of vectors. For a particular track the angle between all consecutive vectors is calculated. Points at the intersection of vectors with angles of less than 15° are removed. The euclidean distance between remaining points is calculated to yield step lengths. Thus a step length is defined as persistent motion without deviation of more than 15°.

Longer step lengths indicate tracks that move in a persistent direction, while short step lengths indicate frequent turns (greater than 15 degrees). Tracks with a more symmetrical, closer to Gaussian, distribution of step lengths indicate Brownian motion which achieves a more thorough search of a local area, while a more skewed step length distribution is indicative of a Lévy walk which searches more broadly.

While Fig. 3 and Fig. 4 show data from only one LN, we increase our statistical power by repeating our hot spot analysis independently for each of 41 experimental observations of LN. The threshold for hot spots is specific to each observation because it depends on the number and initial location of T cells in each LN. We find that 14 of those 41 observations contain hot spots. We analyse the movement of the 514 hot T cell tracks, with 15,717 positions, in all 14 of those observations and 4,998 cold cell tracks, consisting of 157,193 positions, in Fig. 5.

Fig. 5 shows the distribution of step sizes for hot and cold T cell tracks. While the mean step length is similar for both classes of T cells, there is more skew in the cold tracks, suggesting more Lévy-like movement in cold tracks and more thorough Brownian search in hot tracks. The statistical differences between hot and cold T cell tracks are summarized in Table 1: the variance, skew and kurtosis of hot track step lengths are significantly smaller than the 95% confidence interval of cold track step lengths, indicating more Brownian motion in hot tracks.

Brownian motion around the hot spots is also suggested visually in Fig. 4. However not all T cells that visit hot spots have searched thoroughly. Instead, several relative straight paths are visible through the hot spots. Some of those cells travel straight into the hot spots and then search more thoroughly, and others appear to pass through the hot spots without stopping. Additionally, there are other locations not near identified hot spots where cells move in more Brownian motion. Thus, while there appears to be a trend toward more Brownian motion near hot spots, T cell tracks move in various ways, both near hot spots and away from hot spots.

3.2 Analysis of iAnt Robot Movement

While our analysis suggests more Brownian motion of T cells visiting hot spots, some cells in Fig. 4 wander across the hot spot with more persistent directional motion. To calibrate our hot spot detection approach, and to better understand how well differences in movement can be resolved, we conduct similar analysis of simulated iAnt robot data in which we can identify locations with search targets, and we can identify different behavioral states that govern movement.

Fig. 2B shows the distribution of the number of iAnt visits to each location in space: most cells are visited by only 1 iAnt, but a very small number of cells are visited by 5 or 6 iAnts. The distribution is highly skewed, similar to the distribution of T cell visits in Fig. 3B. The distribution of simulated non-adaptive T cells in Fig. 3A is also skewed, but less so.

Figures 6 and 7 show analysis of iAnt robot movement as they search for resources in their environment. In Fig. 6, we show locations visited by iAnts, in this case using a heatmap with red and yellow sites visited by the most iAnts, and blue and green sites visited by fewer iAnts. Superimposed on top of these hot spots are the clusters of tags for which the iAnts were searching.

Fig. 7 shows the step length distribution of iAnts as they search for targets using two different correlated random walk (CRW). Fig. 7 panel A shows iAnts searching in locations known to have resources (informed iAnts using Eqn. 3) while

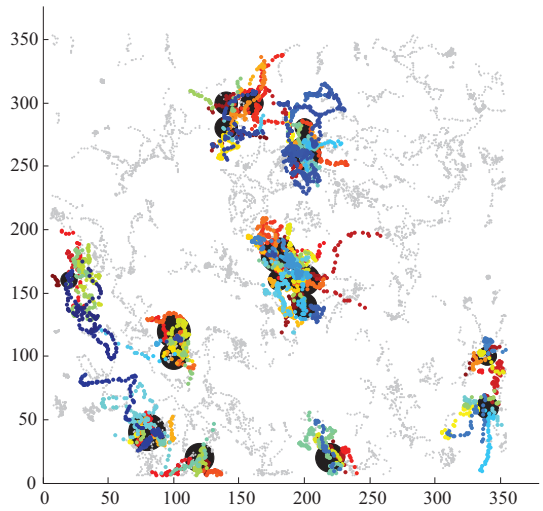

Figure 4: T cell tracks and hot spots from one observed LN. Black circles show hot spots, with circle size indicating the number of unique T cell tracks that visit that location. 124 T cells that visit hot spots are shown in colours (each track a different color) and 313 T cells that do not visit hot spots are shown in gray.

panel B shows iAnts searching at random without any information about resource locations (uninformed iAnts moving according to Eqn. 2).

For iAnts the difference in movement patterns between informed and uninformed search is evident in the statistically lower mean and median of the step length distribution (summarized in Table 2.) While informed iAnts take smaller steps, unlike T cells, the shape of the distribution is not different – the variance, skew and kurtosis of the step lengths of informed iAnts are within the 95% CI of uninformed iAnts.

Thus, iAnts that visit hot spots and T cells that revisit resource locations have different movement than iAnts and T cells that don't visit hot spots or known resource locations. However iAnts and T cells both differ in the distribiution of steps. In T cells this is reflected int the more Gaussian distribution of steps with a higher mean step length which in iAnts the step lengths become shorter.

4. CONCLUSIONS

We have identified hot spots as locations in the lymph node (LN) that are visited by T cells more often than would be expected by chance. T cells that visit those hot spots move differently: the distribution of step lengths is more normally distributed, indicative of more Brownian motion, while distribution of step lengths for other T cells is more skewed (potentially indicative of a Lévy walk) so that there is a greater chance of T cells taking a long step in a persistent direction. The more Brownian motion of T cells that visit hot spots may indicate more thorough local search, while the heavier-tailed distributions of T cells that do not visit hot spots suggests that those T cells move more broadly, perhaps searching for dispersed targets. These results demonstrate that T cells react to their environment in non-random ways,

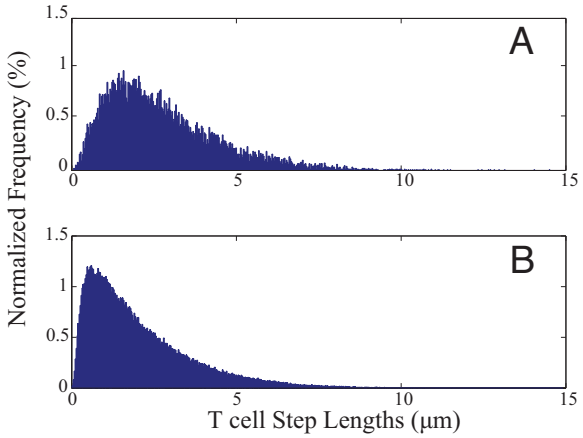

Figure 5: A) Step length distribution for T cell hot tracks and B) cold tracks.

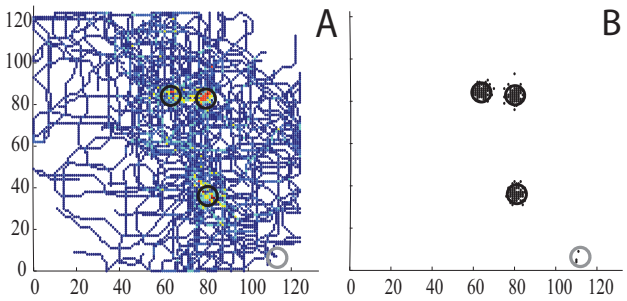

Figure 6: iAnt Search Pattern. A) iAnt tracks of six robots searching for tags. Blue spots were visited by 1 robot, red spots by 6 robots. B) The location of target clusters. Black circles indicate exploited targets. The grey circle correponds to a target cluster that was encountered but not exploited. Grid units are 8 cm.

and more specifically, they suggest that T cells that visit hot spots search more thoroughly.

The differences in the statistical properties of steps produced by T cells visiting hot spots and those that do not, suggest that T cells may adapt to an external cue in the environment to modify their search pattern. It is possible that T cells search more thoroughly when coming into direct contact with a dendritic cell (DC) or an high endothelial venule (HEV) (around which DCs tend to be clustered [8]), or they may respond to a chemical signal or chemokine released by DCs, HEVs or some other feature of the LN.

Given that T cells are selected to repeatedly contact DCs, and that DCs are often clustered in space (likely near the HEVs through which T cells enter the LN [8]), T cells that search areas with DCs more thoroughly may have more repeated contacts as well as contacts with more DCs.

An alternative explanation for hot spots could be that T cells are tracking fibroblastic reticular cells (FRCs), however, the more Brownian search around these points suggests that the tracks are searching thoroughly, not travelling along structures in the LN.

Our hypotheses about T cells are supported by our analysis of the movement of iAnt robots. iAnt movement is

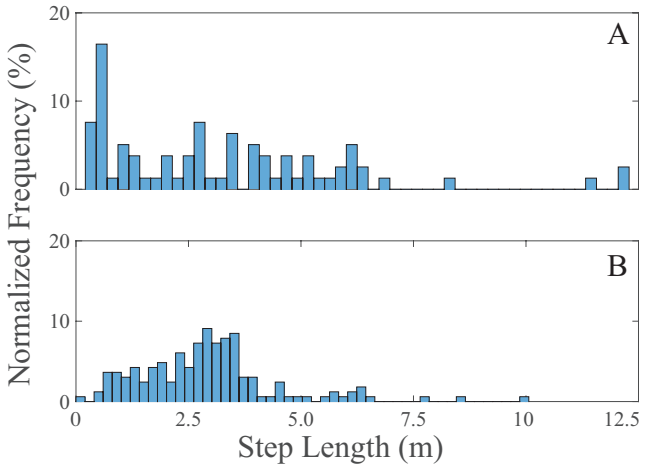

Figure 7: A) iAnts that are re-visiting previously identified tag locations. B) Step length distribution for iAnts that are searching randomly without information about previously identified tag locations. Each histogram divides the region between the minimum and maximum values into 50 equally spaced bins. The bar heights correspond to observed frequency normalized so that the sum over bars equals 100%. .

governed by a set of ant-inspired search behaviours, with parameters tuned by a genetic algorithm (GA) to maximize the collection of resources [14]. In the experiments we analyse here, resources are clustered (in Fig. 6, in 4 large clusters) to mimic the clustered DCs targets of T cells. We validate the method of inferring target locations by correctly inferring the locations of iAnt robots using methods similar to those we use to infer T cell hot spots (Fig. 4). In addition to knowing a priori the location of target locations, we also know more about how iAnt movement behaviours adapt to their environment. iAnts are programmed to use an informed correlated random walk (CRW) with lower correlation among successive step directions when the iAnt is returning to a known target cluster location. This results in a different mean and median step length for informed vs uninformed iAnts (Fig. 7).

The nature of the adaptive movement in iAnts (lower mean and median step lengths for informed iAnts) is different than the hypothesized adaptation in hot T cell tracks (less skew in the distribution of step lengths indicating more Brownian search). However, in both cases, the informed iAnts and the hot T cell tracks appear to search more thoroughly then their uninformed counterparts.

This similarity in search behaviour between iAnts and T cells is noteworthy. iAnts were designed to mimic biological behaviours of foraging ants. Moses and Banerjee have suggested similarities in how ants and T cells search [18]. Despite differences in the search environments and the sensing abilities of the search agents, both T cells and iAnts change their movement in response to features of their environment. T cells (evolved by natural selection to find antigen-bearing DCs) and iAnts (evolved by GAs to collect targets) change their movement patterns to search more thoroughly when targets are nearby.

We identified hot spots in only 34% of our experiments, and in those experiments approximately 25% of T cells visited those locations. These are likely underestimates for two reasons. First, our test identifying hot spots is conservative–only those locations that were visited more frequently than by chance were identified as hot spots, but some locations with fewer visits could be clusters of DCs that happened not to be visited by many T cell tracks. Additionally, only a small number of T cells could be visualized during the experiments. Therefore there may be many more T cells overlapping in space than the ones we have identified. Not visualizing a hot spot may simply be a byproduct of the low density of T cells. In future experimental work we will identify DCs and T cells in the same lymph node to test our ability to identify hot spots.

Another limitation of our computational approach is that it may be difficult to clearly distinguish movement behaviours of T cells visiting hot spots, simply because many T cells move in variable ways–sometimes taking long persistent directional steps and sometimes searching thoroughly. Even for iAnts, which are specifically programmed to search more thoroughly where hot spots are identified, the difference in step distribution is difficult to detect statistically. While there is a clear shift in the average step length of informed iAnts, there is a broad range of steps lengths (up to 12 m) in informed and uninformed iAnts. Our prior experiments [6] show that an adaptive walk with small changes in turning angles (and therefore small changes in the step length distribution) can make a large difference (42.9%) in search efficiency. This suggests that subtle differences in T cell movement might generate important differences in how rapidly T cells encounter DCs.

Our T cell experiments also suggest new strategies for iAnt robots. It is possible that different T cells have different movement patterns, not necessarily because of reactions to the environment. Our iAnts are all programmed identically, and vary in response to information about the environment. The variability in T cell behaviour suggests that it is worth testing variation in search strategies among iAnts. Additionally, some have proposed that T cells move using a Lévy walk [9]. Prior analysis suggests that T cell movement is heavy-tailed (if not strictly Lévy) [6]. A heavy-tailed step distribution vs more Brownian motion (Fig. 5) provides an alternative model for thorough vs extensive search. One advantage of this approach over the current iAnt model described by Hecker at al. [10] (which increases turning angles of successive steps to achieve more thorough search) is that a Lévy-like walk might be tuned with fewer parameters. Additionally, there is substantial mathematical analysis of Lévy walk efficiency that may allow iAnts to tune their search based on analytical predictions of the most efficient walk for a given environment, without needing to evolve. Thus T cells may provide a simpler model of movement that may be more analytically tractable than the current iAnt central place foraging algorithm (CPFA).

Here we have identified similarities and differences in search behaviours of iAnts and T cells. Our analysis provides a computational hypothesis: that hot spots are locations of DC clusters or signaling molecules and that T cells adapt movement in response to sensing those environmental cues. Our future work will test this hypothesis experimentally by simultaneously visualizing fluorescent DCs and T cells in the same ex vivo LN. As we learn more about how T cells move and adapt as they search the LN environment, we can generate new iAnt search strategies to mimic these T cell search strategies. This will continue the cycle of computa-

tional analysis informing experimental design, and experimental observation informing our understanding of T cell search processes. As we improve our understanding of how T cells search, we identify additional mechanisms that computational approaches can emulate.

References

[1] E. U. Acar, H. Choset, Y. Zhang, and M. Schervish. Path planning for robotic demining: Robust sensor-based coverage of unstructured environments and probabilistic methods. *The International Journal of Robotics Research*, 22(7-8):441–466, 2003.

[2] E. J. Allenspach, P. Cullinan, J. Tong, Q. Tang, A. G. Tesciuba, J. L. Cannon, S. M. Takahashi, R. Morgan, J. K. Burkhardt, and A. I. Sperling. Erm-dependent movement of cd43 defines a novel protein complex distal to the immunological synapse. *Immunity*, 15(5):739–750, 2001.

[3] U. Alon, M. G. Surette, N. Barkai, and S. Leibler. Robustness in bacterial chemotaxis. *Nature*, 397(6715):168–171, 1999.

[4] A. Be'er, S. K. Strain, R. A. Hernández, E. Ben-Jacob, and E.-L. Florin. Periodic reversals in paenibacillus dendritiformis swarming. *Journal of bacteriology*, 195(12):2709–2717, 2013.

[5] T. Flanagan, K. Letendre, W. Burnside, G. Fricke, and M. Moses. Quantifying the effect of colony size and food distribution on harvester ant foraging. *PloS one*, 7(7):e39427, 2012.

[6] G. M. Fricke, F. Asperti-Boursin, J. Hecker, J. Cannon, and M. Moses. From microbiology to microcontrollers: Robot search patterns inspired by T cell movement. In *Advances in Artificial Life, ECAL*, volume 12, pages 1009–1016, 2013.

[7] G. M. Fricke, F. Asperti-Boursin, J. Hecker, J. Cannon, and M. Moses. Beyond lévy: Efficiency of t cell search in lymph nodes. (In review)

[8] M. Y. Gerner, P. Torabi-Parizi, and R. N. Germain. Strategically localized dendritic cells promote rapid t cell responses to lymph-borne particulate antigens. *Immunity*, 42(1):172–185, 2015.

[9] T. H. Harris, E. J. Banigan, D. A. Christian, C. Konradt, E. D. T. Wojno, K. Norose, E. H. Wilson, B. John, W. Weninger, A. D. Luster, et al. Generalized lévy walks and the role of chemokines in migration of effector cd8+ t cells. *Nature*, 486(7404):545–548, 2012.

[10] J. P. Hecker, K. Stolleis, B. Swenson, K. Letendre, and M. E. Moses. Evolving Error Tolerance in Biologically-Inspired iAnt Robots. In *ECAL 2013*, 2013.

[11] S. M. Hedrick. The acquired immune system-a vantage from beneath. *Immunity*, 21(5):607–616, 2004.

[12] J. H. Huang, L. I. Cárdenas-Navia, C. C. Caldwell, T. J. Plumb, C. G. Radu, P. N. Rocha, T. Wilder, J. S. Bromberg, B. N. Cronstein, M. Sitkovsky, et al. Requirements for t lymphocyte migration in explanted lymph nodes. *The Journal of Immunology*, 178(12):7747–7755, 2007.

[13] N. Humphries, H. Weimerskirch, N. Queiroz, E. Southall, and D. Sims. Foraging success of biological lévy flights recorded in situ. *Proceedings of the National Academy of Sciences*, 109(19):7169–7174, 2012.

[14] J. P. Hecker and M. E. Moses Beyond pheromones: Evolving error-tolerant, flexible, and scalable ant-inspired robot swarms. *Swarm Intelligence*, 9(1), 43–70, 2015.

[15] I. R. Mackay, F. S. Rosen, U. H. von Andrian, and C. R. Mackay. T-cell function and migration - two sides of the same coin. *New England Journal of Medicine*, 343(14):1020–1034, 2000.

[16] M. P. Matheu, I. Parker, and M. D. Cahalan. Dissection and 2-photon imaging of peripheral lymph nodes in mice. *Journal of Visualized Experiments: JoVE*, (7), 2007.

[17] H. P. Mirsky, M. J. Miller, J. J. Linderman, and D. E. Kirschner. Systems biology approaches for understanding cellular mechanisms of immunity in lymph nodes during infection. *Journal of theoretical biology*, 287:160–170, 2011.

[18] M. Moses and S. Banerjee. Biologically inspired design principles for scalable, robust, adaptive, decentralized search and automated response (radar). In *Artificial Life (ALIFE), 2011 IEEE Symposium on*, pages 30–37. IEEE, 2011.

[19] D. W. Stephens and J. R. Krebs. *Foraging theory*. Princeton University Press, 1986.

[20] S. J. Taylor. The hausdorff α-dimensional measure of brownian paths in n-space. In *Mathematical Proceedings of the Cambridge Philosophical Society*, volume 49, pages 31–39. Cambridge Univ Press, 1953.

[21] G. Viswanathan, F. Bartumeus, S. V Buldyrev, J. Catalan, U. Fulco, S. Havlin, M. Da Luz, M. Lyra, E. Raposo, and H. Eugene Stanley. Levy flight random searches in biological phenomena. *Physica A: Statistical Mechanics and Its Applications*, 314(1):208–213, 2002.

[22] E. O. Wilson and B. Hölldobler. The rise of the ants: a phylogenetic and ecological explanation. *Proceedings of the National Academy of Sciences of the United States of America*, 102(21):7411–7414, 2005.

5. ACKNOWLEDGEMENTS

The authors gratefully acknowledge financial support from NSF EF 1038682, DARPA P-1070-113237, NIH 1R01AI097202-01, the Spatiotemporal Modeling Center 1 P50 GM085273, and a James S. McDonnell Foundation grant for the study of Complex Systems. Thanks to the reviewers for many helpful suggestions.